Supporting Information

Photoelectrochemical performance of ligand-free CsPb$_2$Br$_5$ perovskite

Luyao Xu[1], Yu Yang[1], Weihua Wu[1], Chaoguo Wei, Guanying Luo, Zhongnan Huang, Wei Chen*, and Huaping Peng*

Higher Educational Key Laboratory for Nano Biomedical Technology of Fujian Province, Department of Pharmaceutical Analysis, Faculty of Pharmacy, Fujian Medical University, Fuzhou 350108 (P. R. China)

Corresponding author. E-mail address: E-mail: penghuaping@fjmu.edu.cn (H. Peng); chenandhu@163.com (W. Chen)

[1] *These authors contributed equally to this work.*

Table of contents

Experimental sections

Chemicals and materials: Lead bromide ($PbBr_2$, 99.999%) and cesium bromide (CsBr, 99.999%) were purchased from Sigma-Aldrich Co. Ltd. KCl was obtained from Beijing Chemical Reagent Co. (Beijing, China). A 0.1 M phosphate buffer (pH = 7.4) was prepared by mixing a stock solution of Na_2HPO_4 and NaH_2PO_4. All reagents were used without any further purification.

Characterizations: Powder X-ray diffraction (XRD) was applied by using a Bruker D8 Advance X-ray diffractometer with Cu-Kα (λ = 1.5418 Å). The sample nanostructure was investigated by using transmission electron microscopy (TEM, Tecnai G2 F30). Scanning electron microscope (SEM) image was executed with a Nova Nano SEM 230 instrument (FEI CZECH REPUBLIC S.R.O. Company). UV−vis adsorption spectroscopy was applied by using a UH4150 spectrophotometer (Hitachi). The electrochemical tests were conducted by employing a CHI660C electrochemical workstation (Shanghai Chenhua Instrument Co. Ltd., China) with a typical three-electrode cell. Single-crystal X-ray diffraction (SC-XRD) data were collected by applying graphite-monochromatized Mo Kα radiation (λ = 0.71073 Å) at 230.01(10) K using an Agilent SuperNova dual-source diffractometer with an Atlas detector. The Hall effect measurement was carried out using a Lake Shore Accent HL5500 Hall System. The electrochemical tests were carried out using the CHI660C electrochemical workstation.

Single-Crystal X-ray Diffraction: A colorless $CsPb_2Br_5$ crystal was selected for single-crystal XRD analysis. The collection of the intensity data, cell refinement, and data reduction were carried out with the program CrysAlisPro.[1] The structure was solved by the direct method with program SHELXS and refined with the least-squares program SHELXL.[2-3]

Synthesis of the $CsPb_2Br_5$ nanoplatelets: $CsPb_2Br_5$ nanoplatelets were synthesized by employing a solution supersaturated precipitation method, as follows. To begin, 0.1468 g of $PbBr_2$ was added to a single-neck flask with 8 mL of deionized water under the conditions of magnetic stirring at 70 °C for 6 h (i.e., until the $PbBr_2$ was dissolved). Then, the solution was filtered through a 0.22 μm microporous membrane filter as the temperature was maintained. Next, 2 mL of 0.1 M CsBr was injected into the precursor solution. The reaction was magnetically stirred for 30 min at 70 °C in an open-air environment. Subsequently, the solution was allowed to cool in an ice-water bath until precipitated crystals formed; then, the precipitate was extracted after applying centrifugation at 6000 rpm for 5 min. Lastly, the $CsPb_2Br_5$ nanoplatelets were obtained after the precipitate was freeze-dried. The $CsPb_2Br_5$ single crystals were prepared by applying different concentrations of $CsPb_2Br_5$ nanoplatelets (~10 μM) in an aqueous solution.

Preparation of CsPb₂Br₅ nanoplatelet-modified electrode: In this study, a 3 mm diameter glass carbon electrode was employed as the working electrode. Prior to modification, the glassy carbon electrode was cleaned by polishing the electrode surface with Al_2O_3 powder (1.0, 0.3 and 0.05 μm) before subjecting it to an ultrasonic treatment in water and ethanol for approximately 2 min alternately. Then, the cleaned electrode was dried by using nitrogen. Subsequently, 8 mg of the $CsPb_2Br_5$ nanoplatelets was dispersed in 1 mL of ultra-pure water by using an ultrasonic dispersion system. Lastly, 5 μL of the $CsPb_2Br_5$ nanoplatelet solution was dripped on the surface of the clean glassy carbon electrode that was then allowed to dry at room temperature, and the electrode was recorded as $CsPb_2Br_5$ nanoplatelet/glassy carbon electrode.

Photoelectrochemical measurements: The PEC tests were conducted with three-electrode system, wherein the prepared $CsPb_2Br_5$ nanoplatelet electrode served as the working electrode, Pt wire served as the counter electrode, and an Ag/AgCl electrode served as reference electrode. The process of photocurrent detection was carried out under the conditions of a 0.1 M KCl solution (pH 7.0) irradiated with 367.5 ± 2.5-nm-wavelength LED light (10.18 mW cm⁻²) under a bias of −0.4 V vs. Ag/AgCl. Mott-Schottky plots were obtained under the condition of a frequency of 1000 Hz.

Optimization of the reaction conditions. we explored relationship between the crystal composition and the $PbBr_2$/CsBr ratio. The XRD results suggested that as the concentration of the CsBr continue to increase, the perovskite products varied from $CsPb_2Br_5$ to $CsPbBr_3$ and Cs_4PbBr_6 perovskites (Table S1). The concentration of $PbBr_2$ and CsBr to be 6.4 mM and 2 mM, respectively, were finally used to prepare the pure $CsPb_2Br_5$ perovskite. Interestingly, these results indicated that the $CsPb_2Br_5$ has a lower solubility constant than $CsPbBr_3$, thus the $CsPb_2Br_5$ can precipitate first. It could be further demonstrated by the solubility test with the same concentration of $CsPb_2Br_5$ and $CsPbBr_3$ (6.75 µM) in aqueous solution. As expected, we found that $CsPb_2Br_5$ nanoplatelets precipitated immediately, while $CsPbBr_3$ was a homogeneous solution, which also suggested that $CsPb_2Br_5$ has a lower solubility constant than $CsPbBr_3$ (Figure S1). Besides, we also investigated other influencing factors, such as temperature and pH, which have little influence for the generation of the $CsPb_2Br_5$ perovskite. Considering the production of $CsPb_2Br_5$ perovskite, higher temperature was applied in this work.

Table S1 The relationship between the crystal composition and the $PbBr_2$/CsBr ratio.

Concentration of $PbBr_2$ (mM)	Concentration of CsBr (mM)	Perovskite product
6.4	2	$CsPb_2Br_5$
	10	$CsPbBr_3$ and Cs_4PbBr_6
	20	Cs_4PbBr_6
	40	Cs_4PbBr_6
	60	Cs_4PbBr_6
	80	Cs_4PbBr_6
	120	Cs_4PbBr_6
	160	Cs_4PbBr_6
	200	Cs_4PbBr_6

Fig. S1 Solubility photos of $CsPbBr_3$ (left) and $CsPb_2Br_5$ (right).

Table S2 SC-XRD characterization of CsPb$_2$Br$_5$ single crystal.

```
Bond precision:    Pb-Br = 0.0009 A          Wavelength=0.71073

Cell:              a=8.4372(6)      b=8.4372(6)      c=15.0437(14)
                   alpha=90         beta=90          gamma=90
Temperature:       100 K

                   Calculated                Reported
Volume             1070.91(18)               1070.91(15)
Space group        I 4/m c m                 I4/mcm
Hall group         -I 4 2c                   ?
Moiety formula     Br10 Pb4, 2(Cs)           ?
Sum formula        Br10 Cs2 Pb4              Br5 Cs Pb2
Mr                 1893.62                   946.84
Dx,g cm-3          5.872                     5.873
Z                  2                         4
Mu (mm-1)          53.330                    53.331
F000               1576.0                    1576.0
F000'              1547.20
h,k,lmax           10,10,18                  10,10,18
Nref               316                       316
Tmin,Tmax          0.289,0.587               0.176,0.618
Tmin'              0.067

Correction method= # Reported T Limits: Tmin=0.176 Tmax=0.618
AbsCorr = MULTI-SCAN

Data completeness= 1.000          Theta(max)= 26.350

R(reflections)= 0.0314( 310)      wR2(reflections)= 0.1073( 316)

S = 1.243                 Npar= 15
```
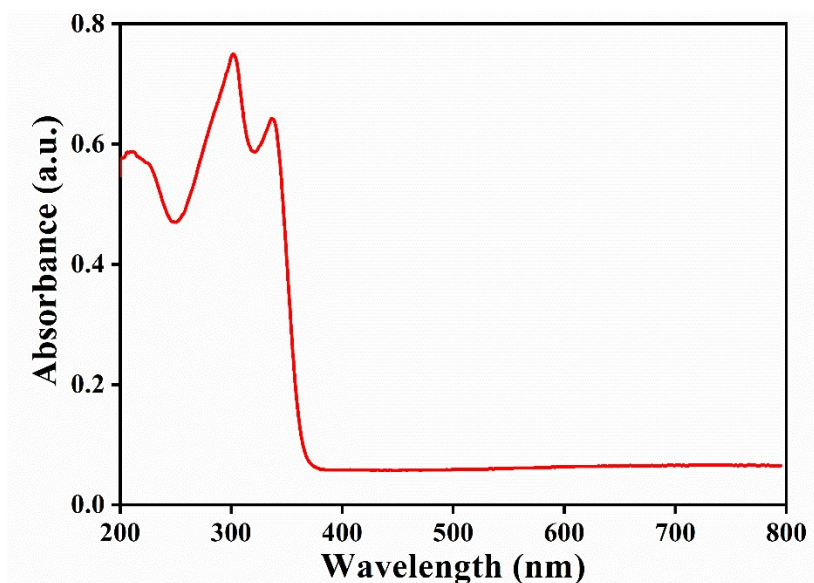
Fig. S2 UV−vis absorption spectrum of CsPb$_2$Br$_5$ nanoplatelets.

The surface morphology of the modified electrodes was investigated by SEM. As shown in Fig. S3, the CsPb$_2$Br$_5$ nanoplatelets modified electrode showed many rectangular sheet structure with the sizes ranging from 5 μm to 20 μm distributed uniformly on the surface of the electrode, which corresponded to the TEM results.
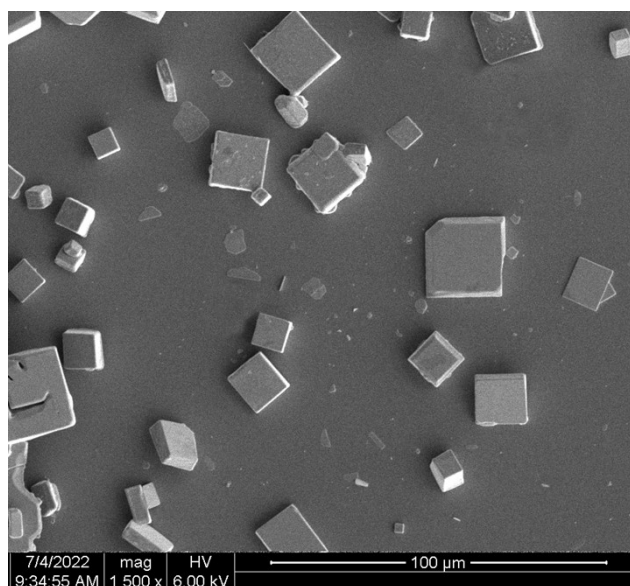
Fig. S3 SEM image of CsPb$_2$Br$_5$ nanoplatelets modified electrode.

Table S3 Comparison of the reported photoelectrochemical performances of all-inorganic cesium halide perovskites systems.

Sample	Electron acceptor/donor	Light intensity (mW cm^{-2})	Photocurrent (μA cm^{-2})	Reference
CsPbBr$_3$ NCs/FTO	—	100	2.25	4
CsPbCl$_3$ NCs/ITO	—	30	0.3	5
CsPbCl$_3$ NWs/ITO	—	30	1.1	5
CsPbBr$_3$ QDs/FTO	—	100	-42	6
CsPbBr$_3$ NCs/FTO	Benzoquinone	100	-40	6
CsPbBr$_2$I NCs/FTO	Benzoquinone	100	-58.8	6
CsPbBr$_{1.5}$I$_{1.5}$ NCs/FTO	Benzoquinone	100	-63.6	7
CsPbBrI$_2$ NCs/FTO	Benzoquinone	100	-36.2	7
Cs$_4$CuSb$_2$Cl$_{12}$ NCs/FTO	—	100	6	8
Cs$_2$PdBr$_6$ NCs /FTO	—	150	1.2	9
Cs$_2$PdBr$_6$ MCs /FTO	—	150	0.33	9
CsPb$_2$Br$_5$ nanoplatelets/glass carbon electrode	—	10.18	8.4	This work

Optimization of conditions for photoelectrochemical performance: The experimental parameters were optimized to obtain the best performance of the $CsPb_2Br_5$ nanoplatelets/Glassy carbon electrode. The irradiation wavelength is a significant factor that is relevant to the photocurrent response. As shown in Fig. S4A, the photocurrent decreased as the exciting wavelength was increased from 365 nm to 940 nm at a definite potential. The highest photocurrent was observed under 367.5 ± 2.5 nm irradiation due to the strong light absorption of $CsPb_2Br_5$ materials. Based on this consideration, 367.5 ± 2.5 nm light was chosen for the best irradiation wavelength.

Applied potential is another important factor relevant to the photocurrent response which would affect the recombination probability of the photo-generated electron/hole pairs. Figure S2B showed that the photocurrent response increased when the negative potential was applied but decreased when the positive potential was applied, indicating that the negative potential will help the separation of electron and holes. Shown in Fig. S4B, the obtained photocurrent quickly decreased when the applied potential was negative than -0.5 V. This may be due to destruction of the structure of $CsPb_2Br_5$ nanoplatelets under negative bias potential. Considering the stability of the electrode and the energy consumption, -0.4 bias-potential was applied in this work.

The pH value of electrolyte solution and the modification amounts of $CsPb_2Br_5$ nanoplatelets were another important factors to affect the photoelectrochemical response. As shown in Fig. S4C, the sensors were tested in a series of KCl aqueous solution with pH ranging from 3.0 ~ 12.0, the maximum photocurrent response appeared at pH of 12.0. In order to ensure the integrity of the material structure as well as obtain a stable photocurrent, pH 7.0 KCl was selected in following measurements. And the photocurrent signal of different concentrations of $CsPb_2Br_5$ nanoplatelets was demonstrated in Fig. S4D. As exhibited, the photocurrent increased until 40 μg $CsPb_2Br_5$ nanoplatelets were dropped on the electrode surface and then decreased rapidly. It could be explained that more electrons were excited with $CsPb_2Br_5$ nanoplatelets concentration increasing, causing the enhancement of the photocurrent density. However, if the $CsPb_2Br_5$ nanoplatelets film too thick, impeding the transfer of the electrons and the effective light harvest, leading to the photocurrent decreased with further increasing. Therefore, 40 μg $CsPb_2Br_5$ nanoplatelets were the optimal.
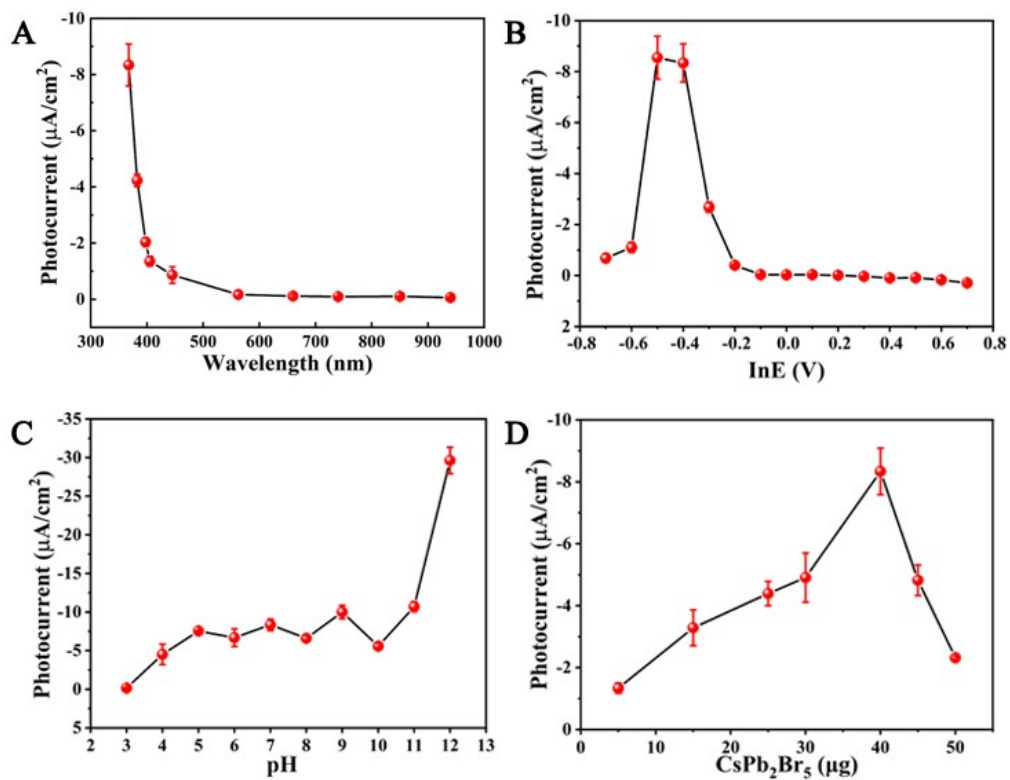
Fig. S4 Optimization of (A) excitation wavelength, (B) the applied potential, (C) pH buffer solution, (D) CsPb$_2$Br$_5$ concentration.

Table S4 Hall effect test parameters of $CsPb_2Br_5$ nanoplatelets films.

	Sample	$CsPb_2Br_5$ nanoplatelets
μ_H	Hall mobility ($cm^2V^{-1}s^{-1}$)	3989
R_H	Hall coefficient ($cm^3\ C^{-1}$)	1.54×10^7

References

(1) CrysAlisPro, Version 1.171.36.28; Agilent Technologies: Santa Clara, CA, 2013.

(2) G. M. Sheldrick, Crystal structure refinement with, *Acta. Crystallogr. Sect A: Found.,* 2008, **64**,112–122.

(3) S. G. Zhao, P. F. Gong, S.Y. Luo, S. J. Liu, L. Li, M. A. Asghar, T. Khan, M. C. Hong, Z. S. Lin, J. H. Luo, Beryllium-free $Rb_3Al_3B_3O_{10}F$ with reinforced interlayer bonding as a deep-ultraviolet nonlinear optical crystal, *J. Am. Chem. Soc.,* 2015, **137**, 2207–2210.

(4) L. Bergamini, N. Sangiorgi, A. Gondolini, A. Sanson, $CsPbBr_3$ for photoelectrochemical cells, *Sol. Energy.*, 2020, **212**, 62–72.

(5) Y. Y. Tang, X. Cao, A. Honarfar, M. Abdellah, C. Chen, J. Avila, M. C. Asensio, L. Hammarström, J. Sa, S. E. Canton, K. Zheng, T. Pullerits, Q. Chi, Inorganic ions assisted the anisotropic growth of $CsPbCl_3$ nanowires with surface passivation effect, *ACS Appl. Mater. Interfaces.*, 2018, **10**, 29574–29582.

(6) Y. F. Xu, M. Z. Yang, B. X. Chen, X. D. Wang, H. Y. Chen, D. B. Kuang, C. Y. Su, A $CsPbBr_3$ perovskite quantum dot/graphene oxide composite for photocatalytic CO_2 reduction, *J. Am. Chem. Soc.*, 2017, **139**, 5660–5663.

(7) M. Z. Yang, Y. F. Xu, J. F. Liao, X. D. Wang, H. Y. Chen, D. B. Kuang, Constructing $CsPbBrxI_{3-x}$ nanocrystal/carbon nanotube composites with improved charge transfer and light harvesting for enhanced photoelectrochemical activity, *J. Mater. Chem. A.*, 2019, **7**, 5409–5415.

(8) X. D. Wang, N. H. Miao, J. F. Liao, W. Q. Li, Y. Xie, J. Chen, Z. M. Sun, H. Y. Chen, D. B. Kuang, The top-down synthesis of single-layered $Cs_4CuSb_2Cl_{12}$ halide perovskite nanocrystals for photoelectrochemical application, *Nanoscale*, 2019, **11**, 5180–5187.

(9) L. Zhou, J. F. Liao, Z. G. Huang, X. D. Wang, Y. F. Xu, H. Y. Chen, D. B. Kuang, C. Y. Su, All-inorganic lead-free Cs_2PdX_6 (X = Br, I) perovskite nanocrystals with single unit cell thickness and high stability, *ACS Energy Lett.*, 2018, **3**, 2613–2619.